

Figure 2. The measured Equivalent Noise Charge (ENC) as a function of the input capacitance (top). The timing resolution as a function of the output pulse amplitude (bottom) [3].

version of the ASIC, a non-negligible disagreement can be observed for the simulated and measured ENC at the lowest peaking time (25 ns) and large values of input capacitance due to an error in the adjustable lead-lag compensation of the front-end amplifier. Another issue was a considerable leakage current from the ElectroStatic Discharge (ESD) protection circuit at the input of the channel [3]. Moreover difference between the theoretical and the measured resolution at 25 ns was observed largely due to the actual peaking time. Though the timing resolution is at the level that satisfies the requirements of the Micromegas and sTGC detectors.

2.1 Testing of Micromegas detectors with VMM1 ASIC

The VMM1 was tested with eight identical $10 \times 10 \text{ cm}^2$ resistive strip micromegas prototypes with 1D readout at the CERN beam facilities as shown in Figure 3. A spatial resolution of $\sim 65 \mu\text{m}$, as shown in Figure 4, has been measured for perpendicular to the detector plane tracks as expected for these detectors [5]. Figure 5 shows the spatial resolution for particle tracks of incident angles $10^\circ - 30^\circ$. The resolution was measured to be $\sim 180 - 120 \mu\text{m}$ respectively. Using the ART signals, the performance of the micromegas detectors was demonstrated to be below 1 mrad as shown in Figure 6. The details of the study above can be found in Ref. [6][7].

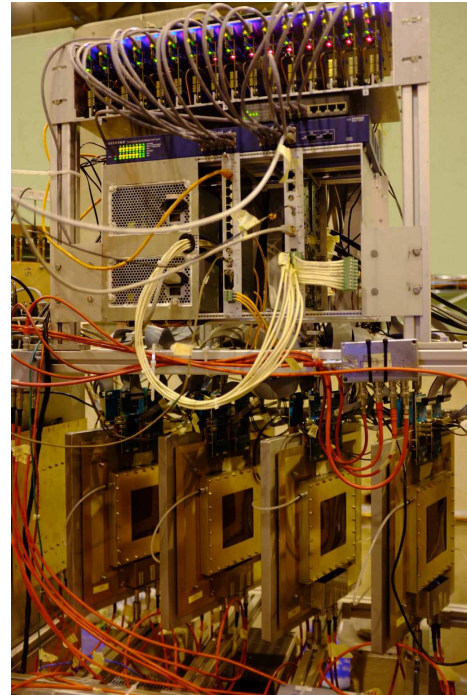


Figure 3. Setup of eight Micromegas detectors at CERN beam line readout by VMM1 [6].

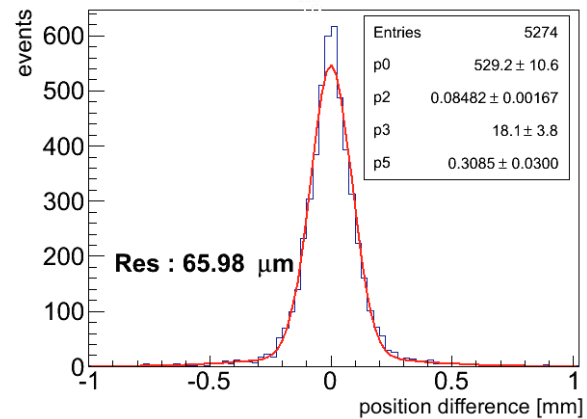


Figure 4. Residual distribution of two micromegas chambers with $400 \mu\text{m}$ strip pitch obtained with charge centroid method. The distribution is fitted with a double Gaussian function. An estimation of the position resolution is extracted by dividing the weighted Gaussian sigmas (p2, p4) with the Gaussian heights (p0, p3) and divide with $\sqrt{2}$. The resolution is demonstrated to be $\sim 65 \mu\text{m}$ [6].

2.2 Testing of sTGC detectors with VMM1 ASIC

In 2014, the full-size sTGC prototype was tested with a high momentum pion beam at the Fermilab test beam facilities. Figure 7 shows the sTGC detector prototype in the middle of the silicon pixel telescope used for external tracking reference. Figure 8 shows the residual distribution with an intrinsic resolution of $\sim 44 \mu\text{m}$ (corrections applied). The details of this study can be found in Ref. [8].

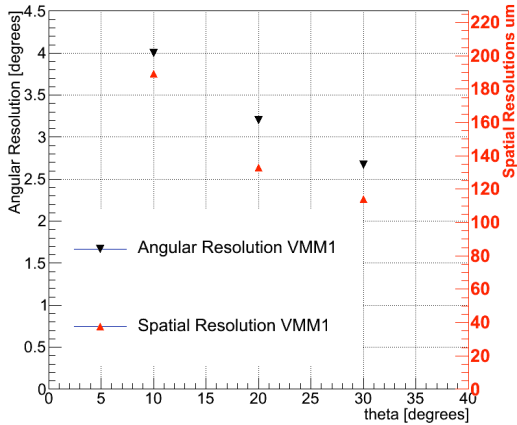


Figure 5. The spatial and angular resolution of a single microegas chamber versus the incident track angle reconstructed using the μ TPC method [6].

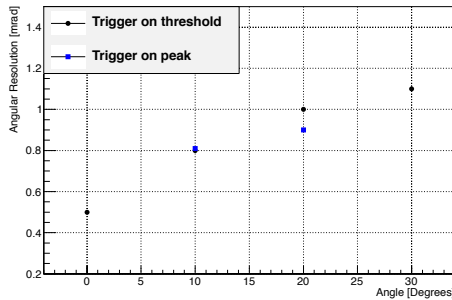


Figure 6. Angular resolution reconstructed with the eight microegas telescope and the ART signals obtained for each of them. For 10° and 20° the ART was measured both in threshold and peak [6].

3 The VMM2 ASIC

The VMM1 ASIC was a successful first version of the VMM ASIC family. For the NSW needs though, a continuous fully digital readout is foreseen. The VMM2 is a deep redesign of the VMM1 correcting the drawbacks found as well as including a fully digital continuous readout mode. Including an order of magnitude transistors per channel more (80 k/ch), VMM2 is as well composed of 64 linear front-end channels. It was fabricated in 2014 in 130 nm Global Foundries 8RF-DM process (former IBM 8RF-DM) and packaged in 400 Ball Grid Array of 1 mm pitch. A block diagram of one of the identical channels is shown in Figure 9. The low-noise charge amplifier with adaptive feedback, test capacitor, and adjustable polarity (to process either positive or negative charge), was optimized for a capacitance of 200 pF and a peaking time of 25 ns. The input MOSFET is a p-channel with gate area of $L \times W = 180 \text{ nm} \times 10 \text{ mm}$ (200 fingers, 50 μm each) biased at a drain current $I_D = 2 \text{ mA}$; this corresponds to an inversion coefficient $IC \approx 0.22$, a transconductance $g_m \approx 50 \text{ mS}$, and a gate capacitance $C_g \approx 11 \text{ pF}$. The filter (shaper) is a third-order designed in delayed dissipa-

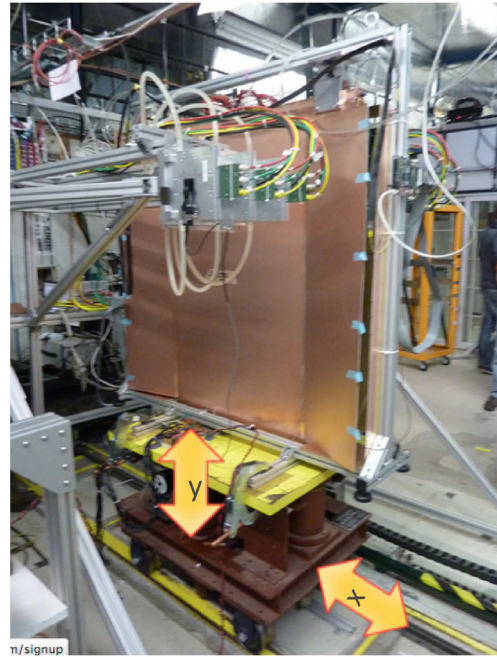


Figure 7. The sTGC prototype detector, inside a copper Faraday cage, in the middle of the silicon pixel telescope [8].

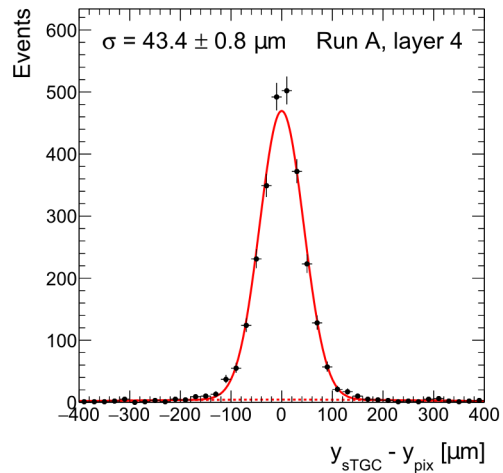


Figure 8. The residual distribution obtained with charge centroid method (corrections are applied) together with the result for the intrinsic resolution [8].

tive feedback DDF [4], has adjustable peaking time in four values (25, 50, 100, and 200 ns) and stabilized, band-gap referenced, baseline. The DDF architecture offers higher analog dynamic range, making possible a relatively high resolution at input capacitance much smaller than 200 pF. The gain is adjustable in eight values (0.5, 1, 3, 4.5, 6, 9, 12, 16 mV/fC).

The peak detector measures the peak amplitude and stores it in an analog memory. The time detector measures the peak timing using a time-to-amplitude converter, i.e., a voltage ramp that starts at the time of the peak and stops at a clock cycle of the BC clock. The Time to Ampli-

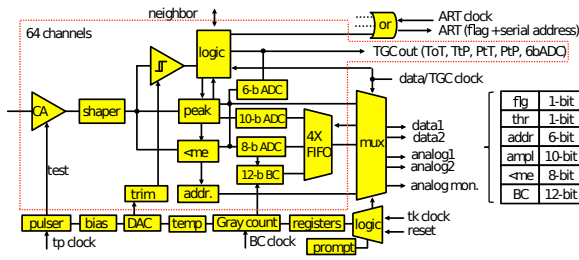


Figure 9. Architecture of VMM2 [10].

tude Converted (TAC) value is stored in an analog memory and the ramp duration is adjustable in four values (60 ns, 100 ns, 200 ns, 400 ns). The peak and time detectors are followed by a set of three low-power ADCs (a 6-bit, a 10-bit, and a 8-bit), characterized by a domino architecture [9] but of a new concept. For the time measurements an additional 12-bit Gray code time-stamp is provided, incremented by an external clock providing 20-bit timing information in total. For each channel, the amplitude measurement by the 6-bit ADC completes the conversion at 25 ns and it is driven as a direct output. These ADCs are enabled depending on the selected mode of operation. The output of the ASIC in digital continuous mode is composed of 38-bits as shown in Figure 9.

Some preliminary measurements of the VMM2 are shown in Figures 10, 11. The ASIC shows good performance with respect to the noise measurements, although the new circuitry shows also some drawbacks. The peak detector, followed by a voltage to current conversion circuitry, shows some bias due to overshoot which results in loosing the ADC precision. Moreover some accumulation in the ADCs was observed.

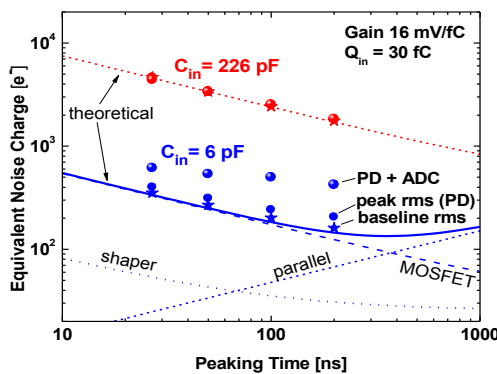


Figure 10. The measured ENC as a function of the peaking time.

The VMM2 ASIC is under testing with and without detectors in several labs and institutes around the world to measure its performance. Moreover all the drawbacks

found until now are fully simulated and corrections have been provided for the next version.

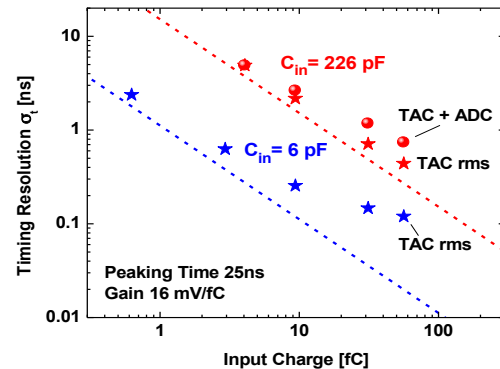


Figure 11. The timing resolution as a function the input charge.

4 Towards VMM3 - Final design

The next version of VMM, the VMM3, will be submitted for fabrication in January 2016. It will be packaged in the same BGA and will provide, in addition to the VMM2 drawbacks corrections, latency and Level-0 buffers necessary for the ATLAS readout. Moreover it will integrate features such as longer TAC ramps, SEU mitigation circuitry as well as handling of higher input capacitance of the order of 1.5 nF needed for the detector elements of NSW.

References

- [1] ATLAS Collaboration, *New Small Wheel Technical Design Report*, ATLAS-TDR-020.
- [2] T. Alexopoulos *et al.* Nuclear Instruments and Methods in Physics Research, **640**, 110 (2011).
- [3] G. De Geronimo, *et al.* IEEE Transactions on Nuclear Science, **60**, 2314 (2013).
- [4] G. De Geronimo and Li Shaorui, IEEE Transactions on Nuclear Science, **58**, 2382 (2011).
- [5] G. Iakovidis, Journal of Instrumentation, **8**, C12007 (2013).
- [6] ATLAS Collaboration, *Performance of the First Version of VMM Front-End ASIC with Resistive Micromegas Detectors*, ATL-UPGRADE-PUB-2014-001
- [7] G. Iakovidis, *Research and Development in Micromegas Detector for the ATLAS Upgrade*, CERN-THESIS-2014-148.
- [8] A. Abusleme, *et al.* arXiv:1509.06329, (2015).
- [9] G. De Geronimo, *et al.* IEEE Transactions on Nuclear Science, **54**, 541 (2007).
- [10] G. De Geronimo, *Readout Electronics for the ATLAS New Small Wheels (Phase 1)*, ACES 2014.